

Hyperellipsoid Density Sampling: Exploitative Sequences to Accelerate High-Dimensional Optimization

Julian Soltes
jsoltes@regis.edu
Regis University
Denver, Colorado, USA

Abstract

The curse of dimensionality presents a pervasive challenge in optimization problems, with exponential expansion of the search space rapidly causing traditional algorithms to become inefficient or infeasible. An adaptive sampling strategy is presented to accelerate optimization in this domain as an alternative to uniform quasi-Monte Carlo (QMC) methods.

This method, referred to as Hyperellipsoid Density Sampling (HDS), generates its sequences by defining multiple hyperellipsoids throughout the search space. HDS uses three types of unsupervised learning algorithms to circumvent high-dimensional geometric calculations, producing an intelligent, non-uniform sample sequence that exploits statistically promising regions of the parameter space and improves final solution quality in high-dimensional optimization problems.

A key feature of the method is optional Gaussian weights, which may be provided to influence the sample distribution towards known locations of interest. This capability makes HDS versatile for applications beyond optimization, providing a focused, denser sample distribution where models need to concentrate their efforts on specific, non-uniform regions of the parameter space.

The method was evaluated against Sobol, a standard QMC method, using differential evolution (DE) on the 29 CEC2017 benchmark test functions. The results show statistically significant improvements in solution geometric mean error ($p < 0.05$), with average performance gains ranging from 3% in 30D to 37% in 10D. This paper demonstrates the efficacy of HDS as a robust alternative to QMC sampling for high-dimensional optimization.

1 Introduction

High-dimensional optimization poses a significant challenge due to the curse of dimensionality (Peng et al., 2023). This is increasingly relevant as big data tasks become more common.

For problems where the global optimum resides within a localized interior region of the parameter space, uniform quasi-Monte Carlo (QMC) methods often prove inefficient (Chen et al., 2025). By sampling uniformly across the entire data hypercube, these methods may consume valuable computational resources exploring irrelevant regions, which can inhibit the identification of global optimal solutions in vast search spaces.

Various approaches have been explored to address this inefficiency, such as modifying traditional optimizers and employing data preprocessing methods (Hinz et al., 2018). This paper presents an alternative: an adaptive sampling strategy informed by the parameter space to intelligently guide the optimizer's search.

The proposed strategy, Hyperellipsoid Density Sampling (HDS), focuses a large initial sample sequence to the target sample size by narrowing the search population to statistically promising regions.

This is achieved by defining multiple hyperellipsoids over the parameter space, with their centers determined by MiniBatchK-Means clustering of an initial Sobol QMC sequence. The number of ellipsoids is found using Agglomerative Hierarchical Clustering, and their axis dimensions are calculated via Principal Component Analysis. Samples are generated within unit hyperspheres using the Marsaglia polar method to ensure angular uniformity, and are subsequently transformed to fit the hyperellipsoids. Any out-of-bounds samples are redistributed using geometric void filling. The result is a non-uniform sample sequence more concentrated in areas likely to contain the global optimum.

For the differential evolution (DE) trials discussed in this paper, it is hypothesized that HDS as an initial sampling strategy will achieve a statistically significant improvement in final solution fitness for high-dimensional evolutionary optimization when compared to QMC sampling methods.

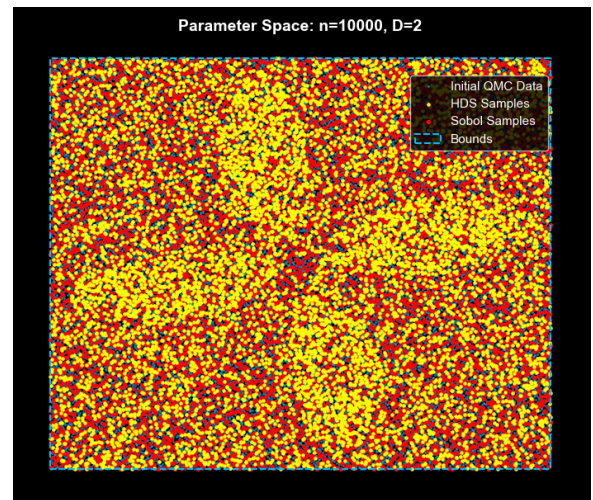


Figure 1: HDS sequence (yellow) and a comparison Sobol sequence (red) for 10,000 samples in 2D.

2 Methodology

2.1 Experimental Methods

This study evaluates the performance of different initial sampling strategies using differential evolution (DE) as the test optimizer. DE is an effective and widely used algorithm for non-differentiable, non-linear, multi-modal, and high-dimensional problems (Stokes et al., 2020). The trials were configured with Scipy Differential Evolution’s default parameters (*strategy = best1bin*, $F = (0.5, 1)$, $CR = 0.7$).

The experimental trials were run against the 29 CEC2017 benchmark test functions, each possessing distinct characteristics to challenge optimizers and are scalable to 10, 30, 50, and 100 dimensions ($D \in \{10, 30, 50, 100\}$). As such, these are the four dimensionalities tested, with bounds of $[-100, 100]$.

50 trials were conducted for two sets of sample sizes, as well as for each combination of test function and dimension, totaling 11,400 DE runs.

The sample sizes tested are 64 and 1000; the lower value is chosen for maximal constraints while providing Sobol its power-of-2 uniformity (Joe & Kuo, 2008). The higher value is chosen to represent a more typical problem.

The maximum number of iterations n_{iter} for the optimization is fixed at 100; this low number was chosen to highlight the practical benefits of HDS with a limited computational budget. The random seed is set to the experimental trial number for both sampling methods, to ensure a fair independent comparison.

The comparison metric used for the analysis is the final solution fitness values for HDS compared to Sobol. Sobol was chosen as the comparison metric due to its high uniformity and low discrepancy in high dimensions (Atanassov & Ivanovska, 2022), as well as its use within the HDS algorithm. Latin Hypercube was considered as an alternative, but does not ensure the same low discrepancy as Sobol in high dimensions (Wang & Sloan, 2007).

To ensure a fair comparison, the geometric mean is used to calculate the average improvement factors for each dimension across all test functions. The optimization run times between the two sampling methods are also compared to assess the impact on overall processing time.

Additionally, the discrepancies of the resulting HDS sequences are compared against Sobol using L2-Star and Centered L2 metrics.

2.2 Hyperellipsoid Density Sampling

The Hyperellipsoid Density Sampling (HDS) method generates N total samples $\mathbf{x} \in \mathbb{R}^D$ within a D -dimensional search space (defined by the bounds \mathbf{B}), using a data-driven approach to focus sample density. The resulting sample distribution is highly non-uniform, increasingly resembling a normal distribution as dimensions scale higher. This is an expected consequence of the algorithm accounting for the curse of dimensionality.

2.2.1 Define Normalized Space. The D -dimensional search bounds, \mathbf{B} , are normalized to the unit hypercube $[0, 1]^D$ to simplify clustering and Principal Component Analysis (PCA).

2.2.2 Generate Initial QMC Sequence. A large initial set of N_{init} samples is generated, where N_{init} is set to the smallest power of 2 greater than or equal to $200 \cdot D$, ensuring sufficient coverage that

scales with dimensionality as $N_{init} = 2^{\lceil \log_2(200 \cdot D) \rceil}$. This value is capped at 2^{15} by default for efficiency.

These values balance computational efficiency with spatial discrepancy for high sample sizes and dimensions, as well as ensuring power-of-2 QMC sample sizes for maximum uniformity. The initial QMC samples are generated using a Sobol sequence within the normalized unit hypercube. This initial set serves as the basis for determining the geometry of the search space.

2.2.3 Gaussian Weights (Optional). If prior information (such as target distribution or optimal solution region) is known, Gaussian weights may be applied to the initial QMC samples to influence their distributions. As a result, the final sample locations are shifted towards the desired region. An example of an HDS sample sequence with weights applied is shown below.

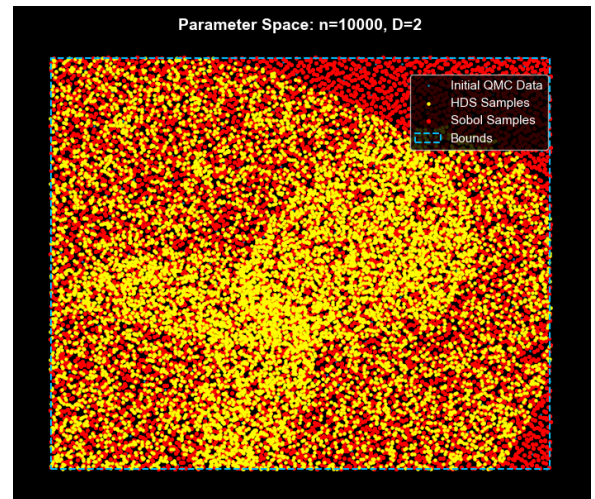


Figure 2: 2D HDS sequence with weights applied towards $x = 0.25$, $y = 0.25$, for bounds of $[0, 1]^D$

2.2.4 Initial KMeans Centroid Estimation. The initial N_{init} samples are clustered using MiniBatchKMeans to reduce the data into a smaller, computationally efficient set of K_{init} centroids (defaulted at 100), simplifying the subsequent hierarchical analysis. MiniBatchKMeans is used in place of standard KMeans to minimize sample generation time.

The value $K_{init} = 100$ was chosen as a stable value, as it provides the optimal balance between spatial information and computational efficiency. This value consistently generates clear KMeans and Hierarchical clustering results to sufficiently cover the parameter space while minimizing the high overhead of the linkage calculation. As dimensionality approaches $1000D$, this default value is scaled down proportionally, ensuring the final sample distribution remains minimally affected.

2.2.5 Identify Number of Ellipsoids (K). Agglomerative Hierarchical Clustering (AHC) is performed on the K_{init} centroids. The optimal number of clusters, K , is determined by analyzing the dendrogram’s linkage matrix (Fig. 3) and selecting a cut-off distance δ corresponding to the largest dissimilarity between the clusters. This

distance threshold determines the final number of clusters, which in turn defines the number of ellipsoids used in the subsequent calculations.

Due to the stochastic nature of the initialization process, the optimal cluster count K may vary across multiple sample generations with identical input parameters. The number of ellipsoids can also be provided as an input parameter, and the AHC calculations will be skipped.

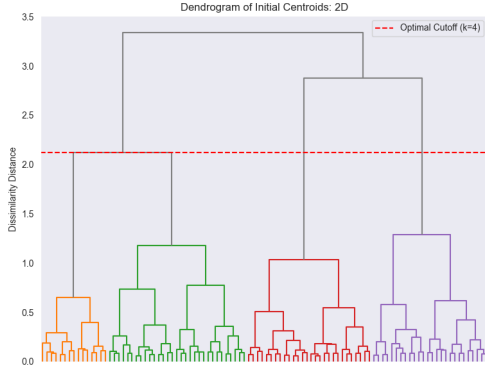


Figure 3: Dendrogram used to identify number of ellipsoids for a representative 2D sample sequence.

2.2.6 Final Ellipsoid Centroids. A final MiniBatch-KMeans fit, using the optimal cluster count K , assigns each of the N_{init} samples to one of K clusters, yielding the \mathbf{c}_k cluster centers (origins) and the sample counts n_k for clusters $k = 1, 2, \dots, K$.

2.2.7 Hyperellipsoid Geometry. The shape and orientation of the K hyperellipsoids are defined using PCA on the samples within each cluster.

For each cluster k , the origin of the hyperellipsoid is set to the centroid \mathbf{c}_k . PCA is performed on the associated samples, \mathbf{s}_k . The principal components define the orientation of the ellipsoid axes, \mathbf{P} . The length of the i -th semi-axis, $\sigma_{i,k}$, is determined by the calculated variance $\text{Var}_{i,k}$ along that component:

$$\sigma_{i,k} = \sqrt{\text{Var}_{i,k} + \epsilon}$$

where ϵ is a small scalar added for numerical stability in case of zero variance.

2.2.8 Allocate Samples. The total number of required samples, N , is distributed among the K hyperellipsoids based on the relative size of their initial clusters. The number of samples allocated to cluster k , N_k , is

$$N_k = \text{round} \left(N \cdot \frac{n_k}{\sum_{i=1}^K n_i} \right)$$

where n_k is the number of initial QMC samples belonging to cluster k .

2.2.9 Initialize Unit Hypersphere Samples. For each cluster k , a set of direction vectors \mathbf{u} on the surface of the unit sphere is generated using the Marsaglia polar method. Each sample vector \mathbf{s} is normalized to a unit length \mathbf{u} by dividing by its L2-norm:

$$\mathbf{u} = \frac{\mathbf{s}}{\|\mathbf{s}\|}$$

where \mathbf{s} is an initial vector with D standard normal components.

2.2.10 Radial Scaling Factor. A global scaling factor λ is applied to all hyperellipsoid axes to control the spread of the sampling points. This factor is calculated by scaling the square root of the χ^2 critical value with an empirically tuned, dimension-variant constant C_D .

The confidence level of the χ^2 critical value is chosen as $\alpha = 0.9999$ to capture the majority of a cluster's variance. The empirically tuned constant C_D is a function of the dimension D :

$$C_D = 0.55 - 0.01 \cdot \ln(D)$$

The final global scaling factor λ is then defined as:

$$\lambda = C_D \cdot \sqrt{\chi_{\alpha,D}^2}$$

This scaling is critical; a factor that is too small or too large leads to a high rejection rate of generated samples (described below). A 2D example is shown below, generated with a reduced λ for visual clarity of the geometry.

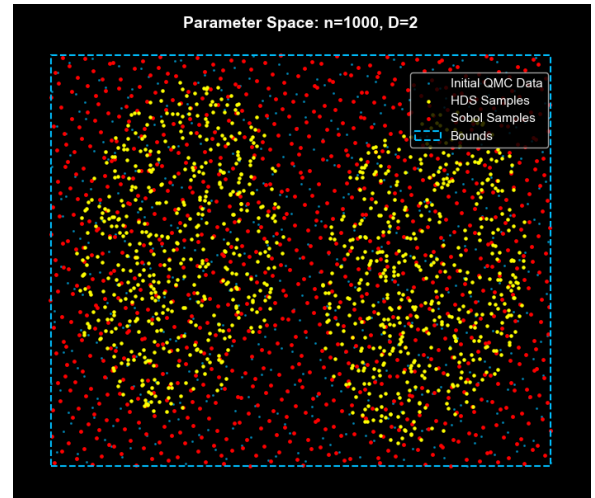


Figure 4: HDS samples in 2D for number of ellipsoids $K = 2$, using a reduced radial scaling factor to easily visualize the geometry.

2.2.11 Apply QMC Radial Scaling. To ensure a uniform distribution throughout the hypervolume, the radial distance ρ is determined using a 1D Sobol sequence $q \in [0, 1]$. This radial scaling factor ρ is then applied to the unit direction vector \mathbf{u} :

$$\mathbf{u}_{\text{scaled}} = \mathbf{u} \cdot (q^{1/D} \cdot \lambda)$$

Where the term $q^{1/D}$ ensures that the radial distances are uniformly distributed within the hypervolume. The global scaling factor λ is integrated here.

2.2.12 *Transform to Hyperellipsoid.* The scaled unit sphere samples, now a matrix S_{scaled} , are transformed into the final hyperellipsoid by applying the variance-based axis lengths and rotating them back to the original parameter space.

The full transformation, which includes scaling and rotation, is defined by matrix multiplication:

$$\mathbf{X} = S_{\text{scaled}}\Sigma\mathbf{P}^T + \mathbf{C}_k$$

where:

- \mathbf{X} is the matrix of final ellipsoid samples.
- S_{scaled} is the matrix of scaled unit direction vectors.
- Σ is a Diagonal Scaling Matrix where the diagonal elements are $\sqrt{\text{Var}_i + \epsilon}$, representing the scaled axis lengths.
- \mathbf{P}^T is the Rotation Matrix (the transpose of the PCA component matrix \mathbf{P}).
- \mathbf{C}_k is the cluster centroid vector, \mathbf{c}_k , added (broadcast) to every row of the scaled and rotated matrix.

2.2.13 *Boundary Rejection & Void Filling.* Samples generated outside the normalized search bounds $[0, 1]^D$ are rejected. A large number of initial samples is generated to compensate for this expected rejection rate.

If the count of valid samples is less than the target N , the remaining points (N_{void}) are generated using an adaptive void-filling strategy. The method identifies the most sparse regions using the k-nearest neighbor (KNN) distance of the existing HDS samples within a BallTree. The resampled points are then generated using a truncated normal distribution, centered on existing samples in these sparse regions.

This approach ensures the total sample count is met while providing explorative coverage to areas not fully contained by the hyperellipsoids, which was found to significantly improve performance over non-adaptive void-filling methods.

2.2.14 *Denormalization.* If the ‘normalize’ parameter is set to ‘False’, the resulting final HDS sequence \mathbf{H} (which is currently normalized between $[0, 1]$) is scaled back to the original search bounds B using the minimum \mathbf{B}_{min} and range $\Delta\mathbf{B}$ of the original bounds:

$$\mathbf{H}_{\text{final}} = \mathbf{H} \odot \Delta\mathbf{B} + \mathbf{B}_{\text{min}}$$

where \odot denotes the element-wise Hadamard product. This yields the final HDS sequence.

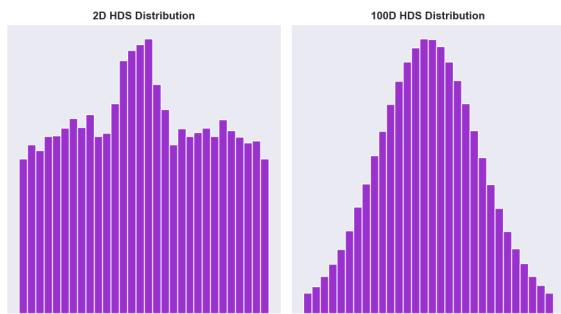


Figure 5: Sample distributions for HDS sequences in 2D (left) and 100D (right).

3 Results

3.1 Optimization Fitness

The final solution fitness being minimized is used as the metric to compare optimization efficacy of HDS compared to QMC sampling. The analysis is performed on the differential evolution results from the 50 independent trials, for each of the 2 sample sizes, 4 dimensions and 29 CEC2017 benchmark test functions.

The experimental trials on the benchmark functions revealed that HDS consistently outperformed the Sobol QMC in all of the tested dimensions. The 95% confidence intervals show similar performance between the sampling methods in lower dimensions (10D, 30D), whereas in higher dimensions (50D, 100D) the CI_{95} ranges do not fall below 1.0x improvement factors. This highlights the consistent improvements of HDS in higher-dimensional problems.

The $N = 1000$ trials saw an overall geometric mean improvement factor of 1.15x, implying HDS averages 15% improved final fitness values across all dimensions. A summary of the geometric mean fitness improvement across various dimensions is presented in Table 1.

The $N = 64$ trials showed similar but more nuanced improvements, struggling to show statistical significance in 10D and 100D. The 10D case specifically showed a 3% decrease in solution quality compared to Sobol, with highly variable performance leading to a p value of 0.15.

As shown in the figure below, HDS achieved statistically significant improvements in average solution fitness across all tested dimensions in the $N = 1000$ trials, as well as most dimensions in the $N = 64$ trials.

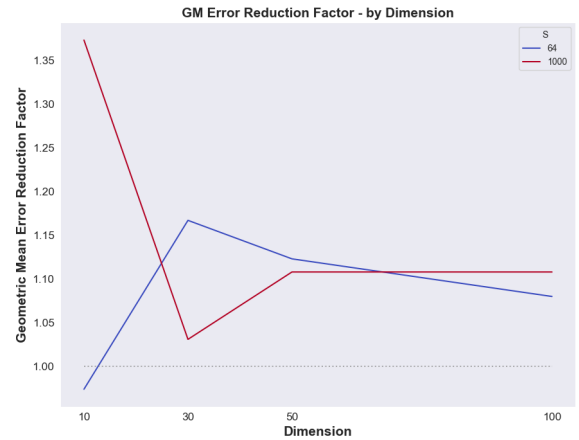


Figure 6: HDS vs Sobol geometric mean final solution improvement factor, by dimension, for sample sizes 64 and 1000.

3.2 Computational Efficiency

The multiple machine learning model fits and backend QMC generations naturally lead to slower sample generation than a single deterministic QMC method such as Sobol or Latin Hypercube.

The sample generation time increases with sample size and dimension (Table 2, Table 3, Fig. 7). Optimization run time $Ratio_{Time}$,

Table 1: Final Solution Quality

Samp.	D	HDS Err.	Sobol Err.	Ratio	p -Val	CI_{95}
1000	10	6.0×10^{-1}	8.3×10^{-1}	1.37	3×10^{-2}	(0.92, 2.05)
1000	30	6.7×10^3	6.9×10^3	1.03	1×10^{-4}	(0.89, 1.19)
1000	50	5.2×10^4	5.7×10^4	1.11	4×10^{-5}	(1.06, 1.15)
1000	100	5.8×10^5	6.4×10^5	1.11	4×10^{-6}	(1.06, 1.15)
64	10	8.9×10^0	8.7×10^0	0.97	1.5×10^{-1}	(0.67, 1.43)
64	30	1.1×10^4	1.2×10^4	1.17	3×10^{-5}	(1.05, 1.30)
64	50	7.5×10^4	8.4×10^4	1.12	1×10^{-6}	(1.07, 1.18)
64	100	8.5×10^5	9.2×10^5	1.08	1.6×10^{-1}	(1.04, 1.13)

highly influenced by sample generation time in this low-iteration domain, is shown in Table 4.

The overall average run time ratio is found to be $Ratio_{Time} = 0.951$, with a p value below 6×10^{-292} . The results show that the HDS trials were 4.90% slower overall for the 1000 sample size trials. This run time ratio takes into account the sample generation time for both methods. For the 64 sample size trials, the lower optimization time becomes dominated by the sample generation time. Full optimization run time values by dimension are shown in Fig. 8 and Table 4.

It is worth noting that for higher number of evolution iterations than tested in these trials ($n_{iter} > 100$), the sample generation time will occupy a smaller fraction of the overall optimization time.

Due to the scaling of sample generation time, HDS sequencing for high dimensions ($D > 1000$) and sample sizes ($N > 10,000$) may be computationally prohibitive. However, in this domain, the increased computational overhead of initializing a single sequence may be small compared to overall optimization time.

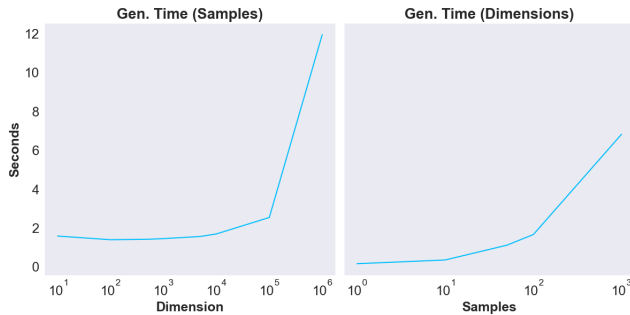


Figure 7: Sample generation times by dimension (left) and sample size (right).

3.3 Discrepancies

HDS inherently sacrifices uniformity due to its exploitative nature. This is explored by quantifying the discrepancies of HDS and pure Sobol sequences.

Higher L2-Star discrepancy values are an expected trade-off of the algorithm’s less uniform focus; as such, the L2-Star discrepancies for HDS are lower than those of Sobol. The Centered L2, however, is much lower in the HDS sequences due to the tighter

Table 2: Generation Time by Sample Size (100D)

n_{samples}	Avg Time (s)	Std Dev (s)	CI_{95}
10	1.59	0.45	(1.46, 1.72)
100	1.40	0.24	(1.33, 1.47)
500	1.42	0.19	(1.37, 1.48)
1000	1.46	0.20	(1.40, 1.51)
5000	1.57	0.28	(1.49, 1.65)
10000	1.70	0.27	(1.62, 1.78)
100000	2.54	0.29	(2.46, 2.63)
1000000	11.95	0.91	(11.69, 12.21)

Table 3: Generation Time by Dimension (N = 1000)

Dimensions	Avg Time (s)	Std Dev (s)	CI_{95}
1	0.166	0.034	(0.156, 0.176)
10	0.358	0.126	(0.322, 0.394)
50	1.118	0.213	(1.057, 1.178)
100	1.667	0.298	(1.582, 1.752)
1000	6.826	0.601	(6.656, 6.997)

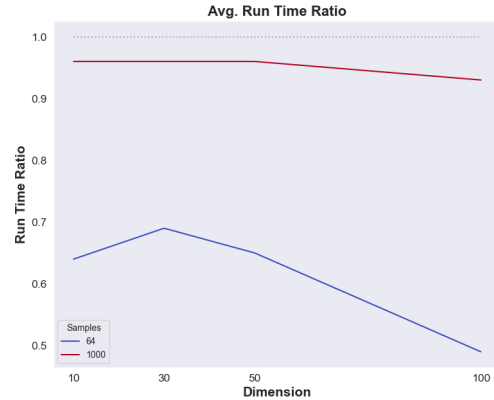


Figure 8: Ratio of Sobol and HDS DE full optimization run times for 64 and 1000 samples.

clustering of samples. Together this implies high local uniformity, with lower global uniformity across the full parameter space.

For a set of 30 representative 100-dimensional trials, the discrepancy comparisons using L2-Star and Centered L2 metrics are shown in Fig. 9 and Table 5, below.

4 Ease of Use & Implementation

Hyperellipsoid Density Sampling is designed to generate samples with the same minimal inputs required of standard QMC sequences, making it seamlessly integratable with existing workflows.

Table 4: Run Time Ratio Comparison

<i>Samples</i>	<i>D</i>	<i>Ratio_{time}</i>	<i>p</i> -Value
1000	10	0.96	3.7×10^{-12}
1000	30	0.96	9.9×10^{-52}
1000	50	0.96	6.7×10^{-87}
1000	100	0.93	9.9×10^{-171}
64	10	0.64	5.5×10^{-195}
64	30	0.69	1.3×10^{-186}
64	50	0.65	8.8×10^{-215}
64	100	0.49	6.5×10^{-233}

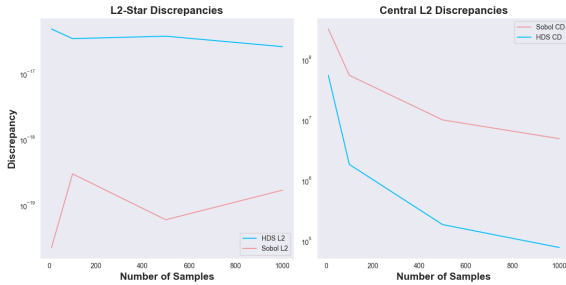


Figure 9: L2-Star (left) and Centered L2 (right) Discrepancies for HDS and Sobol, for a fixed 100D.

Table 5: Discrepancies

<i>N</i>	L2-Star ($\times 10^{-17}$)		Centered-L2 ($\times 10^4$)	
	HDS	Sobol	HDS	Sobol
10	48	0.000023	5500	32000
100	34	0.000300	180	5500
500	37	0.000060	19	1000
1000	26	0.000170	8	490

HDS is implemented as a streamlined Python package, following the conventions of Scipy’s QMC module. It uses a small set of standard library imports for minimal external dependency. The open-source code is available at [github.com/jgsoltes/Hyperellipsoid-Density-Sampling] for full use and reproducibility.

5 Conclusion

This study establishes Hyperellipsoid Density Sampling (HDS) as a robust and highly effective initial sampling strategy for high-dimensional optimization problems. HDS leverages unsupervised learning to bypass complex high-dimensional geometric calculations, generating a non-uniform sample sequence that effectively exploits statistically promising regions of the parameter space. The experimental results consistently show that HDS leads to statistically significant improvements in final solution quality compared to standard uniform Sobol quasi-Monte Carlo (QMC) sequences on the CEC2017 benchmark test functions.

HDS demonstrated substantial performance gains across 50 independent trials. Across all tested dimensions, the overall geometric mean improvement factor compared to Sobol was $1.15\times$ (an average 15% gain in solution quality), achieved with a favorable run time ratio of $0.95\times$ (only a 5% increase in total computational time). The performance ranged from a high of 37% improvement in $10D$ ($p = 0.03$) to a low of 3% in $50D$ ($p = 1 \times 10^{-4}$). The efficacy of HDS highlights the value of using a non-uniform approach to focus computational resources on regions more likely to contain global optima.

The core mechanism of HDS—manipulating sample density based on learned or prior knowledge—is broadly applicable. This density control feature, particularly through the optional Gaussian weights, is a key benefit that extends the utility of HDS beyond traditional optimization. This method can provide a focused, denser sample distribution beneficial in various non-parametric domains, including complex data modeling, experimental design, sensitivity analysis, and the training of deep learning or reinforcement learning models. HDS presents a powerful and robust alternative to QMC methods, particularly when facing high-dimensional search spaces.

6 Future Works

Future works include exploring the performance of HDS against a wider range of optimization algorithms and test functions, as well as unconstrained problems, to validate its robustness.

Many components of the HDS workflow are derived empirically. A more rigorous mathematical framework may be explored such that the high-dimensional geometry is utilized for more elegant and efficient sample generation.

Further research would focus on rigorously defining the parameters, such as initial QMC sample size, number of initial estimation clusters, as well as miscellaneous constants and scaling factors. This would also include optimizing the algorithm’s sample generation time, especially for high sample counts and dimensions $D \gg 100$ and $N \gg 10,000$.

The trials in this study were conducted without using Gaussian weights. Evaluating the impact of these weights on problems where prior information about the optimal solution location is known would validate the effectiveness of this weighting strategy.

Additionally, hybrid sampling-optimization strategies can be explored. This may include an initial optimization initialized with uniformly distributed samples, followed by a second optimization using HDS to exploit the newfound regions of interest.

Acknowledgments

The author would like to thank Dr. Ksenia Polson, Dr. Kellen Sorauf, Dr. Mike Busch, and Monet Morris for their invaluable feedback and support throughout this study. It would not have been possible without the insights gained from each of our discussions.

This research was conducted independently and was not part of a formal project.

References

- [1] Emil Atanassov and S. Ivanovska. 2022. On the Use of Sobol' Sequence for High Dimensional Simulation. In *Lecture Notes in Computer Science*. 646–652. doi:10.1007/978-3-031-08760-8_53
- [2] Jian Chen, Hui Jiang, and Nicholas Kirk. 2025. High-Dimensional Quasi-Monte Carlo via combinatorial discrepancy. *arXiv.org* (2025). arXiv:2508.18426 <https://arxiv.org/abs/2508.18426> Preprint submitted August 25, 2025.
- [3] Thies Hinz, Nestor Navarro-Guerrero, Sebastian Magg, and Stefan Wermter. 2018. Speeding up the hyperparameter optimization of deep convolutional neural networks. *International Journal of Computational Intelligence and Applications* 17, 02 (2018), 1850008. doi:10.1142/s1469026818500086
- [4] Stephen Joe and F. Y. Kuo. 2008. Constructing Sobol Sequences with Better Two-Dimensional Projections. *SIAM Journal on Scientific Computing* 30, 5 (2008), 2635–2654. doi:10.1137/070709359
- [5] Mohammad Z. Naser, Mohammed K. Al-Bashiti, Abdul T. G. Tapeh, Ammar Naser, V. Kodur, Rami Hawileeh, Jaafar Abdalla, Nasim Khodadadi, Amir H. Gandomi, and Alireza Dehghan Eslamlou. 2025. A review of benchmark and test functions for global optimization algorithms and metaheuristics. *Wiley Interdisciplinary Reviews Computational Statistics* 17, 2 (2025). doi:10.1002/wics.70028
- [6] Dong Peng, Zhiwei Gui, and Haijun Wu. 2023. Interpreting the Curse of Dimensionality from Distance Concentration and Manifold Effect. *arXiv.org* (2023). arXiv:2401.00422 <https://arxiv.org/abs/2401.00422> Preprint submitted December 31, 2023.
- [7] Zoe Stokes, Arghya Mandal, and W. K. Wong. 2020. Using Differential Evolution to design optimal experiments. *Chemometrics and Intelligent Laboratory Systems* 199 (2020), 103955. doi:10.1016/j.chemolab.2020.103955
- [8] Xiaoqun Wang and Ian H. Sloan. 2007. Low discrepancy sequences in high dimensions: How well are their projections distributed? *J. Comput. Appl. Math.* 213, 2 (2007), 366–386. doi:10.1016/j.cam.2007.01.005